HHS Public Access

Author manuscript

*J Orthop Res*. Author manuscript; available in PMC 2015 June 18.

Published in final edited form as:

*J Orthop Res*. 2009 June ; 27(6): 833–840. doi:10.1002/jor.20769.

# Remodeling of Murine Intrasynovial Tendon Adhesions following Injury: MMP and Neotendon Gene Expression

**Alayna E. Loiselle**[1], **Gwynne A. Bragdon**[1], **Justin A. Jacobson**[1], **Sys Hasslund**[1,3], **Zenia E. Cortes**[1], **Edward M. Schwarz**[1], **David J. Mitten**[1], **Hani A. Awad**[1,2], and **Regis J. O'Keefe**[1]

[1]Department of Orthopaedics, The Center for Musculoskeletal Research, University of Rochester —Box 665, 601 Elmwood Avenue, Rochester, New York 14620

[2]Department of Biomedical Engineering, University of Rochester, Rochester, New York

[3]Department of Orthopedics, Aarhus University Hospital, Aarhus, Denmark

## Abstract

Tendon injury frequently results in the formation of adhesions that reduce joint range of motion. To study the cellular, molecular, and biomechanical events involved in intrasynovial tendon healing and adhesion formation, we developed a murine flexor tendon healing model in which the flexor digitorum longus (FDL) tendon of C57BL/6 mice was transected and repaired using suture. This model was used to test the hypothesis that murine flexor tendons heal with differential expression of matrix metalloproteases (MMPs), resulting in the formation of scar tissue as well as the subsequent remodeling of scar and adhesions. Healing tendons were evaluated by histology, gene expression via real-time RT-PCR, and in situ hybridization, as well as biomechanical testing to assess the metatarsophalangeal (MTP) joint flexion range of motion (ROM) and the tensile failure properties. Tendons healed with a highly disorganized fibroblastic tissue response that was progressively remodeled through day 35 resulting in a more organized pattern of collagen fibers. Initial repair involved elevated levels of *Mmp*-9 at day 7, which is associated with catabolism of damaged collagen fibers. High levels of *Col3* are consistent with scar tissue, and gradually transition to the expression of *Col1*. *Scleraxis* expression peaked at day 7, but the expression was limited to the original tendon adjacent to the injury site, and no expression was present in granulation tissue involved in the repair response. The MTP joint ROM with standardized force on the tendon was decreased on days 14 and 21 compared to day 0, indicating the presence of adhesions. Peak expressions of *Mmp-2* and *Mmp-14* were observed at day 21, associated with tendon remodeling. At day 28, two genes associated with neotendon formation, *Smad8* and *Gdf-5*, were elevated and an improvement in MTP ROM occurred. Tensile strength of the tendon progressively increased, but by 63 days the repaired tendons had not reached the tensile strength of normal tendon. The murine model of primary tendon repair, described here, provides a novel mechanism to study the tendon healing process, and further enhances the understanding of this process at the molecular, cellular, and biomechanical level.



*Correspondence to:* Regis J. O'Keefe (T: 585-273-5630; F: 585-756-4727; regis_okeefe@urmc.rochester.edu).

Additional Supporting Information may be found in the online version of this article.

**Keywords**

flexor tendon healing; matrix metalloproteases; adhesions; mouse model; biomechanics

Tendon is a specialized tissue that undergoes almost frictionless excursion to mediate skeletal movement. Traumatic injury to the flexor tendons result in abundant scar formation as well as the formation of adhesions that impair tendon function. The molecular events involved in flexor tendon repair remain largely unknown, as this complex process involves coordinated interactions of multiple cells and tissues. In this regard, animal models of tendon may provide essential insights that cannot be inferred solely from clinical observations. Animal studies have shown that tendon repair is mediated by “intrinsic” cells (e.g., epitenon and endotenon cells)[1–3] and “extrinsic” cells (e.g., synovial sheath cells and inflammatory cells such as macrophages) that aid in the initial repair, but are also implicated in adhesion formation.[1,4]

Animal models of flexor tendon healing, including canine, chicken, rabbit, rat, and mouse,[5–10] among others, have provided an excellent screening tool for experimental flexor tendon therapies that led to improved clinical outcomes.[5,6] Large animal (e.g., canine) studies have influenced clinical practice by demonstrating the importance of controlled passive motion (CPM) for adhesion-free tendon healing.[5,6] However, it is still common for primary tendon repairs to endure complications that prevent or delay restoration of appropriate functional ability, even with the application of CPM-based rehabilitation programs, which underscores the importance of understanding the molecular basis of this clinical problem.[11]

The mouse model offers a potentially powerful tool to elucidate the molecular events involved in repair because of the availability of transgenic mouse models of gain and loss of function. For example, a mouse model of inducible TGF-β deficiency has recently been used to investigate the role of TGF-β signals in flexor tendon healing.[12] However, a thorough evaluation of flexor tendon healing in wild-type mice using a comprehensive assessment approach will offer tremendous value in guiding experiments that use mouse models of gain and loss of function. While murine models of Achilles tendon healing have been established,[12–14] it is necessary to have a separate model of flexor tendon healing due to the differences in anatomy and cellular environment,[15] as well as clinical problems associated with adhesion formation that do not occur in extrasynovial tendons. Recent work has shown that the anatomy of the mouse hind paw is similar to zone II in the human hand and, as such, is a good model to study flexor tendon healing and adhesion formation.[16]

In this study, we present an in vivo mouse model of primary flexor digitorum longus (FDL) tendon repair of a fully transected tendon. To test the hypothesis that murine flexor tendons heal with differential expression of matrix metalloproteases (MMPs), resulting in the formation of scar tissue as well as the subsequent remodeling of scar and adhesions. We performed histological analyses to document the characteristics of the different phases of healing as well as real-time RT-PCR and in situ hybridization to assess the temporal and spatial patterns of genes involved in repair and remodeling over a period up to 35 days post-injury. In addition, we examined the functional properties of the repaired tendon including

the flexion range of motion (ROM) of the metatarsophalangeal (MTP) joint and the tensile biomechanical properties up to 63 days post-repair.

## MATERIALS AND METHODS

### Tendon Repair Surgery

Approval was obtained from the University Committee on Animal Research. Six-to-eight-week-old female C57BL/6 mice (Jackson Laboratories, Bar Harbor, ME) were anesthetized by intraperitoneal injection of 4 mg/kg xylazine and 60 mg/kg ketamine. The right plantar paw and medial hind limb were shaved and prepared with alcohol and betadine. Under magnification, a longitudinal incision was made starting from the base of the digits of the plantar hind foot and extending proximally to the mid-postero-medial calf. The distal FDL tendon was exposed and two horizontal 8-0 nylon sutures in a modified Kessler pattern were placed in the intact tendon. The tendon was then transected between the sutures and repaired by approximating the transected ends using the suture. The tendon was also transected proximally along the tibia at the myotendinous junction to protect the repair. The skin was closed with running 4-0 nylon sutures. The mice were returned to their cages and allowed free active motion and weight bearing following recovery from anesthesia. On days 3, 7, 10, 14, 21, 28, and 35 post-repair, animals were sacrificed and the tendons were harvested for histological analysis ($N = 5$ repairs per time point and 5 age-matched contralateral sham specimens per time point), in situ hybridization, and RNA extraction ($N = 5$ repairs per time point). Specimens for biomechanical testing were harvested at 0, 14, 21, 28, 42, and 63 days post-repair ($N = 8–10$ repairs per time point with age matched contralateral sham specimens harvested from each mouse at each time point).

Sham surgeries were performed on control groups. Identical anesthesia and exposure were performed. When the distal FDL tendon was isolated, two horizontal 8-0 sutures in a modified Kessler pattern were sutured through the tendon. This suture was then removed without transecting the tendon. However, the proximal FDL tendon was released at the myotendinous junction as in the repair group. The skin was closed with running 4-0 nylon sutures.

### Histology

For tendon harvest, skin was removed from the entire hind limb leaving all subcutaneous tissues intact. Meticulous dissection of the surgical site was performed under magnification. En bloc resection of the injury site and surrounding soft tissues was undertaken. The surgical site was not violated. Sham specimens were also harvested at each time point.

The harvested tendon and surrounding tissues were fixed in 10% formalin, processed, and embedded in paraffin. Three-micron sections were prepared and stained with Alcian Blue/Hematoxylin and OrangeG using standard techniques.

### Quantification of Relative Granulation Tissue and Tendon Tissue Area

Three sections from each of the five specimens at each time point were analyzed in a blinded fashion for the relative area of tendon tissue and granulation tissue. ImageJ software

(http:// rsb.info.nih.gov/ij/) was used to trace the area of granulation tissue, and the tendon tissue separately. The percentage of each tissue type was calculated based on the sum of the total area measured. A one-way ANOVA with Tukey post-test was used to determine significant differences in the relative area of granulation tissue or tendon tissue at each time point post-repair, and a *t*-test was used to determine if there was a significant difference between granulation tissue and tendon tissue at a given time point.

### RNA Extraction and Real-Time RT-PCR

Repaired tendons were harvested from the distal aspect of the tarsal tunnel up until the tendon bifurcated into the digits. Tendons were then homogenized in Trizol reagent (Invitrogen, Carlsbad, CA) using the Ultra Turrax T8 homogenizer (IKA Works, Wilmington, NC). Total RNA was isolated from a pooling of five repaired tendons per time point using Trizol reagent according to manufacturer's protocol. One microgram of RNA was reverse-transcribed using M-MLV Reverse Transcriptase (Invitrogen) following the manufacturer's protocol. Briefly, RNA was denatured at 70°C for 5 min, 200 U of MMLV reverse transcriptase enzyme were used in a final reaction volume of 20 μl. One microliter of cDNA was used for Real-Time RT-PCR using SYBR Green (Applied Biosystems, Foster City, CA) and specific primers for mouse *Cola11*, *Col3a1*, Matrix metalloproteases *2*, *9*,*14*, *Scleraxis*, *Gdf-5*, *Smad8*, and *Cox-2* (Table 1). The PCR was carried out using the RotorGene Real-Time DNA amplification system (Corbett Research, Sydney, Australia). Gene expression was normalized to β-*actin*. Gene expression data was assessed beginning with day 3 post-injury specimens due to the relative metabolic inactivity of normal tendon tissue.

### In Situ Hybridization

Specific probes for *Col1a1*, *Col3a1* (kindly provided by Dr. Eero Vuorio),[17] and *Scx* (kindly provided by Dr. Andrew Lassar) were used. Anti-sense probes were labeled using MAXIscript In vitro Transcription Kit (Ambion Inc., Austin, TX) according to the manufacturer's protocol. Briefly, 1 μg of linearized cRNA was transcribed in the presence of 50 μCi [$^{33}$P] UTP (Amersham, Piscataway, NJ) at 37°C for 20 min. Template DNA was then digested with TURBO DNase at 37°C for 15 min. The transcript was purified using a MicroSpin G-50 column (Amersham) and the amount of radiolabeled RNA incorporation was determined. Paraffin embedded tendon sections were prepared using mRNA *locator* (Ambion Inc.) according to manufacturer's protocol. Briefly, slides were dewaxed and incubated at 58°C overnight with 100 μl hybridization buffer and probes. The sections were covered with salinized coverslips to maintain moisture. Slides were washed at 55°C with 4× SSC/1 mM DTT, 2× SSC/1mM DTT, nonspecifically bound probe was hydrolyzed using RNase A, and the sections were further washed in 2× SSC/1mM DTT, 0.1× SSC. Autoradiography was performed using Kodak film (Rochester, NY) and slides were dipped in Kodak emulsion and exposed for 7–21 days. Darkfield and brightfield images were obtained and processed as previously described.[18]

## Adhesion Testing

Immediately following sacrifice, the lower hind limb was disarticulated from the knee and the proximal FDL tendon along the tibia was released just proximal to the tarsal tunnel without disrupting the skin at the ankle or foot. The proximal end of the tendon was secured between two square pieces of tape using a thin layer of cyanoacrylate. The lower hind limb was fixed in a custom apparatus where the tibia was rigidly gripped to prevent rotation. To standardize the neutral position, the toes were passively extended by the examiner and allowed to return to an unloaded position before a digital image was taken medially to determine the neutral position (zero load) of the MTP joint. The FDL tendon was incrementally loaded in the same anatomical direction as flexor muscle line of force using dead weights that were statically suspended from a hook and line passing through the proximal FDL tendon/tape composite. The dead weights were suspended for 30 s before the digital pictures were taken to avoid creep effects. With each increment of load, a digital image was taken to quantify the MTP flexion angle relative to the neutral position. The MTP joint flexion angles were measured from the digital images by two independent observers (J.A.J. and S.H.) using ImageJ software (http://rsb.info.nih.gov/ij/) and plotted versus the applied loads. The flexion data were fitted to a single-phase exponential association equation of the form: MTP Flexion Angle = $\beta \times [1 - \exp(-m/\alpha)]$; where m is the applied load (Prism GraphPad 3.0, GraphPad Software, Inc., San Diego, CA). The curve fit was constrained to the maximum flexion angle ($\beta$) for normal tendons that was previously determined to be 75° for the maximum applied load. The constant $\alpha$ (Adhesion Coefficient) governing the rate of rise of the flexion curve with loading was determined as previously described[19] by nonlinear regression as a measure of the resistance to MTP flexion due to impaired gliding. In addition, the MTP flexion ROM was determined as the flexion angle corresponding to the maximum applied load of 19 g.

## Biomechanical Testing

Following the MTP flexion test, the proximal extent of the FDL tendon was released at the tarsal tunnel, with dissection medially along the bone. Once the tendon was free from the tunnel, the calcaneus was removed, freeing the proximal end of the tendon for direct gripping in the mechanical testing apparatus as described.[19] The distal bones of the foot were directly gripped in custom grips without disrupting the repair or the branching tendon insertion into the phalanges. The specimen was placed in sterile gauze soaked with saline to maintain adequate tissue hydration until tested. The FDL tendon was then mounted on the Instron 8841 DynaMight™ axial servohydraulic testing system (Instron Corporation, Norwood, MA) and tested in tension in displacement control at a rate of 30 mm/min until failure. Force-displacement data were automatically logged and plotted and the maximum tensile force and stiffness were determined.

## Statistical Analysis

Data were analyzed using a one-way analysis of variance followed by Bonferroni's multiple comparisons with a significance level of $\alpha = 0.05$. Repair data were compared to day 0 repaired tendons. Maximum tensile force at day 63 was also compared to day 42 repairs for statistical significance. MTP ROM, tensile force, and stiffness are presented as percentage of

normal un-operated tendon to show the changes that occur in healing tendons compared to the properties of normal tendon.

## RESULTS

### Histological Analysis of Healing

To histologically assess the progression of tendon healing, the distal FDL tendons of C57Bl/6 mice were iatrogenically lacerated and repaired. The repaired tendons were then harvested at multiple times up to 35 days post-injury and processed for histology. Shamoperated tendons (which only involved creating an incision and isolating the distal FDL tendon without laceration) were similar to un-operated control tendons at all time points. These tendons were composed of an epitenon layer that was 1–2-cells-thick surrounding bundles of collagen organized in a parallel manner with tenocytes distributed throughout the tendon (Fig. 1A). Three days after repair, a few inflammatory cells could be observed to have invaded the repair site (Fig. 1B). On day 7, extensive fibroblast-like cell proliferation could be observed originating along the surface of the tendon in the tenosynovium, and the cells in the thickened epitenon had proliferated and begun to form an external callus tissue that mimics fracture healing (Fig. 1C). By 10 days, there was increased cellularity at the injury site and the external callus increased in size (Fig. 1D). On day 14, a thick callus of cells had bridged the injury site and begun to invade and replace the adjacent tendon ends (Fig. 1E). On day 21, the repair site encompassed a highly disorganized fibroblastic tissue with abundant remodeling evident in regions adjacent to the injury site that extended throughout the original tendon tissue (Fig. 1F). By this time, the width of the repaired tendon was nearly double the width of uninjured tendon, and the collagen fibers were highly disorganized. On day 28, there was progressive tendon remodeling as the tendon width decreased and the collagen fibers were better organized and began to orient parallel to the long axis of the tendon (Fig. 1G). On day 35, the tendon continuity was restored, the collagen fibers were organized in a dense parallel arrangement, and the cellularity of the repaired tendon was dramatically decreased (Fig. 1H).

Repaired flexor tendons initially had a minimal cellular response, followed by a steady increase in granulation tissue area. The amount of granulation tissue steadily increased to day 10 post-repair, at which time the difference between granulation tissue and tendon tissue was greatest. As healing progressed, the cellularity of the repair decreased and was replaced by collagen fibers. The amount of tendon tissue surpassed the area of granulation tissue at 21 days post-repair (Fig. S5).

### Clinical Observations

Active motion of the toes is observed at 24–28 days postrepair. By day 35, there are no apparent functional difficulties of the foot.

### Temporal Expression of Genes during Tendon Repair

We assessed the mRNA expression levels for a panel of genes that play different roles in inflammation, repair, and remodeling. Since COX-2 is a potent mediator of inflammation that induces MMPs, we examined mRNA expression of *Cox-2, Mmp-2, Mmp-9, and*

*Mmp-14*. The initial phase of healing within the first 3 days after injury was associated with elevated levels of *Cox-2* gene expression (Fig. S1A) that remained elevated for the first 10 days of healing but decreased significantly by 14 days and continued to decrease thereafter ($p < 0.05$). *Mmp-9* expression peaked on day 7, reaching a 15-fold increase compared to day 3 expression levels ($p < 0.05$; Fig. 2A), but then quickly decreased by day 10 and thereafter. Interestingly, expression levels of *Mmp-2* and *Mmp-14* were significantly delayed, compared to *Mmp-9*, as they peaked on day 21 and remained elevated through day 35. *Mmp-2* was 3–5-fold greater on days 7 through 14, then peaked to greater than 10- fold on day 21 compared to day 3 expression levels. Similarly, between 7 and 14 days, *Mmp-14* expression levels were 7-fold greater than day 3 and increased to more than 16-fold on day 21 (Fig. 2C, D).

Substantial changes in matrix gene expression were observed as early as 7 days following injury. The expression of *Col3* peaked on day 10 (7.7-fold increase compared to day 3) which gradually decreased thereafter (Fig. S1B). In contrast, *Col1a1* peaked on day 14 (13.3-fold increase compared to day 3), and remained elevated (greater than 5-fold) up to 35 days post-injury (Fig. S1C).

We also examined the expression of *Gdf-5* and *Smad8*, two genes involved in neotendon formation.[20,21] *Gdf-5* was expressed at low levels during the first 3 weeks of healing, but by day 28 there was a fourfold increase in expression (Fig. 2E). Similarly, the *Gdf-5* responsive transcription factor, *Smad*,[22] was increased 76-fold on day 28 and 89-fold on day 35 (Fig. 2F). The elevation of these transcription factors might be indicative of the transition toward a more organized tendon structure.

Finally, we examined the expression of *Scleraxis (Scx)*; a basic-Helix-Loop-Helix transcription factor that defines a unique population of cells destined to form tendon and ligament tissue.[23] Interestingly, as early as day 7, there was a significant eightfold increase in the expression of *Scx* compared to day 3, which decreased slightly after 7 days but remained somewhat elevated up to 35 days post-injury (Fig. 2B).

### *Scleraxis, Col1,* and *Col3* Localization during Tendon Repair

While gene expression in healing tendons has been extensively studied, there are no data on the spatial localization of genes during tendon repair. Control tendon had no detectable expression of *Scx* (Fig. 3A). However, in response to the injury, *Scx* expression was markedly increased in the tendon adjacent to the site of injury. In contrast, the granulation tissue had no detectable expression of *Scx*. Maximal expression of *Scx* was present 7 days after repair and then declined over time towards basal levels, consistent with the real-time RT-PCR expression patterns (Fig. 3D, E). By day 21 and thereafter, *Scx* expression was decreased to basal levels in the remodeled tendon (Fig. 3F).

Since type III collagen is typically synthesized by fibroblasts and is characteristically expressed in healing granulation tissue as a rapid response to injury, we examined the spatial expression of *Col3a1* over time by in situ hybridization. On day 7 post-injury, a high level of expression of *Col3a1* was localized in the proliferative fibroblastic granulation tissue adjacent to the injury site. No expression was observed in the tendon proper throughout (Fig.

S1B). On day 10, *Col3a1* continued to be strongly expressed in the reparative tissue (Fig. S1C). Consistent with the real-time RTPCR data, *Col3a1* expression was reduced on day 21 (Fig. S1D), with a further decrease on days 28 and 35 (Fig. S1E, F). Interestingly, in sham repair tendon, there was minimal *Col3* expression exclusively in the paratenon (Fig. S1A).

During repair, *Col1* is also confined to fibroblastic granulation tissue, and is absent from the tendon tissue (Fig. S1H). By day 10, the area of *Col1* is greater, consistent with an increase in the amount of fibroblastic tissue at the repair site (Fig. S1I). On day 21, expression of *Col1* is observed in the granulation tissue, but also in the tendon tissue as remodeling of the tendon proceeds (Fig. S1J). A marked decrease in *Col1* expression is observed on days 28 and 35 (Fig. S1K).

### Adhesion and Biomechanical Testing

To assess adhesion formation, we measured the range of the MTP joint flexion ROM (the flexion angle measured upon the application of the maximum load of 19 g in the adhesion test) and the adhesion coefficient (a measure of gliding and flexion resistance over the range of applied loads (0–19 g) in the adhesion test) as previously described.[19] Immediately following surgery at day 0, there was no significant change in the MTP joint ROM or the adhesion coefficient compared to normal un-operated tendon (66.1 ± 9.8 degrees and 7.9 ± 6.4, respectively; mean ± SD).[19] However, by 14 and 21 days, there was a significant 46% and 33% decrease in the MTP joint ROM ($p < 0.05$; Fig. 4). The ROM improved progressively over time such that, by 28 days and thereafter, it was not significantly different than day 0 repairs. Consistent with these observations, the adhesion coefficient at 14 and 21 days post-surgery was threefold and sevenfold greater than day 0, respectively, although these differences were not statistically significant ($p = 0.18$; Fig. S3).

Immediately following the assessment of the MTP joint flexion, the repaired tendons were harvested to measure the tensile strength (as measured by the maximum tensile force) and stiffness (the slope of the linear region of the force-displacement curve) using tensile biomechanical testing. At day 0, tensile strength and stiffness were only 15% and 24% of the normal tendon properties (9.72 ± 1.51 N and 5.14 ± 0.77 N/mm, respectively; mean ± SD; $p < 0.05$).[19] The maximum tensile force and stiffness increased progressively over time and reached 72% and 152% of normal unoperated tendon by 63 days after surgery ($p < 0.05$; Fig. 5; Fig. S4).

## DISCUSSION

Our findings show that tendon healing occurs in a coordinated manner with a unique temporal and spatial pattern of cell and tissue responses and gene expression. The initial repair process is dependent upon the proliferation of fibroblast-like cells derived from the tenosynovium and the formation of an external “healing callus.” These epitenon cells proliferate and form the external healing granulation tissue initially composed primarily of type III collagen with subsequent remodeling and a transition to type I collagen. Although *Scleraxis* expression is increased, its localization is limited to cells located within the injured tendon and is absent from fibroblasts in the healing callus, which is indicative of the formation of a scar tissue healing response rather than a tendon regeneration response.

Progressive healing of the tendon is associated with extensive tissue remodeling and increased levels of *Mmp-2* and *Mmp-14* mRNA expressions. During the late remodeling process, *Gdf-5* and *Smad8* expressions are increased and the tissue becomes more organized and tendon-like in morphology. Interestingly this later remodeling phase is associated with a decrease in tendon adhesions and a return to more normal tendon function.

The pattern of MMP expressions suggests a two-phased response of these genes to tendon repair, consistent with previously presented data in a rat model.[10] *Mmp-9* is secreted by inflammatory cells[24] and the greater than 16-fold induction on day 7 corresponds to the catabolism of damaged collagen fibers at the repair site during initiation of the healing response. The subsequent decrease in *Mmp-9* after 7 days is associated with a profound anabolic phase in which type III collagen and type I collagen are rapidly deposited in an attempt to restore tendon integrity. In healing wounds at skin and other sites of scar formation, type III collagen deposition typically precedes that of type I collagen, since type III collagen is characterized by greater elasticity, and is converted to the stronger, stiffer type I collagen as healing proceeds.[25] Thus, the pattern of tendon healing mimics other scar formation responses. The second phase of MMP expression occurs following restoration of the tendon tissue integrity. Histology and biomechanical data suggest that the healing tendon is functional at 24–28 days post-repair, as indicated by restoration of digital and MTP joint flexion at this time. This return to function is in contrast to our previous work in a model of flexor tendoplasty,[19,26] in which adhesions persist through day 28. This difference is likely to due to differences in the extent of the injuries in these two models. Both *Mmp-2* and *Mmp-14* are elevated 21 days following injury during the tendon remodeling and reorganization phase of healing. The expression pattern suggests that *Mmp-2* and *Mmp-14* are involved in the transition from fibroblastic granulation tissue to a more organized collagen structure.

*Scleraxis*, the so-called tendon-specific basic helix-loophelix transcription factor is thought to be important for tendon formation during embryonic development. *Scleraxis* knockout mice have recently been shown to be viable but have severe tendon defects.[27] Others have demonstrated the confinement of *Scleraxis* expression to the syndetome compartment of the somites that is responsible for formation of the axial tendons.[28] In our study, we observed that *Scleraxis* is induced shortly after tendon injury and during the subsequent repair. However, since *Scleraxis* is induced in tendon cells within the injured tendon but is absent from the fibroblastic granulation tissue that participates in the repair, our findings suggest that tendons heal via a scar formation as opposed to tissue regeneration. The peak of *Scleraxis* expression in the tendon proper on day 7 and the absence of detectable expression in the scar tissue suggest that mature tenocytes within the injury zone respond to the injury, but do not directly participate in tendon regeneration although they may influence progenitor cell differentiation during tendon repair. Subsequent formation of tendon during the late remodeling phases may occur through regulation of other genes. *Tenomodulin*has been shown to be induced by *Scleraxis* in tendon cells.[29] Interestingly, *Scleraxis* expression can also be stimulated by genes involved in tendon development such as *Gdf-5*.[21,30]

*Gdf-5* has been shown to induce ectopic tendon formation,[21] and loss of this gene results in a short-term delay in tendon repair.[13] *Smad8* has also been shown to induce neotendon

formation.[20] The induction of these genes late in the repair process may suggest that they are involved in the transition from a scar-forming wound response to tendon-like tissue. This occurs after initiation of a secondary phase of repair that involves remodeling and replacement of the initial soft tissue-healing callus with more organized tissue composed of type I collagen. While the initial phase of healing is associated with the presence of adhesions, the second phase has improved biomechanical properties and a better tendon gliding function. Thus, a biphasic response to injury is suggested by the gene expression profile, biomechanical data, and gliding coefficient.

Altogether, our experiments define cellular, molecular, and biomechanical events that occur during intrasynovial tendon repair. However, there are several limitations to our study, including the release of the flexor tendon at the myotendinous junction, which is not consistent with clinical practice as well as the possible reaction of the tendon to the suture. Furthermore, while the expression patterns of several genes are presented here, this is not a complete picture of the molecular events involved in flexor tendon healing and adhesion formation. This model does, however, provide a way to test the role of various genes and potential interventions involved in optimal tendon repair.

In summary, flexor tendon repair is characterized by distinct stages of healing that are associated with unique morphological, cellular, and molecular events. While early scar formation appears necessary to stabilize the healing tendon, the adhesions that form as a result of this initial scar formation reduce tendon gliding and joint flexion. This is the major complication observed in flexor tendon primary repair in humans. The current study provides insight concerning the cellular and molecular regulation of flexor tendon and provides potential targets that could be manipulated to reduce adhesion formation.

## Supplementary Material

Refer to Web version on PubMed Central for supplementary material.

## ACKNOWLEDGMENTS

The authors thank Krista Scorsone for technical assistance with the histology, Dr. Paul Kingsley for technical assistance with in situ hybridization, as well as David Reynolds and Tony Chen for technical assistance with biomechanical testing. This work was supported, in part, by research grants from Whitaker Foundation and the Orthopaedic Research Education Foundation (OREF).

## REFERENCES

1. Lilly SI, Messer TM. Complications after treatment of flexor tendon injuries. J Am Acad Orthop Surg. 2006; 14:387–396. [PubMed: 16822886]
2. Lundborg G, Rank F, Heinau B. Intrinsic tendon healing. A. new experimental model. Scand J Plast Reconstruct Surg. 1985; 19:113–117.
3. Mass DP, Tuel RJ. Intrinsic healing of the laceration site in human superficialis flexor tendons in vitro. J Hand Surg [Am]. 1991; 16:24–30.
4. Strickland J. Flexor tendon injuries: I. Foundations of treatment. J Am Acad Orthop Surg. 1995; 3:44–54. [PubMed: 10790652]
5. Gelberman RH, Botte MJ, Spiegelman JJ, et al. The excursion and deformation of repaired flexor tendons treated with protected early motion. J Hand Surg [Am]. 1986; 11:106–110.

6. Gelberman RH, Woo SL, Lothringer K, et al. Effects of early intermittent passive mobilization on healing canine flexor tendons. J Hand Surg [Am]. 1982; 7:170–175.
7. Lou J, Manske PR, Aoki M, et al. Adenovirus-mediated gene transfer into tendon and tendon sheath. J Orthop Res. 1996; 14:513–517. [PubMed: 8764858]
8. Matthews P, Richards H. The repair potential of digital flexor tendons. J Bone Joint Surg [Am]. 1974; 56B:618–625.
9. Potenza AD. Tendon healing within the flexor digital sheath in the dog. J Bone Joint Surg [Am]. 1962; 44-A:49–64.
10. Oshiro W, Lou J, Xing X, et al. Flexor tendon healing in the rat: a histologic and gene expression study. J Hand Surg [Am]. 2003; 28:814–823.
11. Green, DP.; Hotchkiss, RN.; Pederson, WC. Green's operative hand surgery. 4th ed. New York: Churchill Livingstone; 1999. p. v
12. Battaglia TC, Clark RT, Chhabra A, et al. Ultra-structural determinants of murine Achilles tendon strength during healing. Connect Tissue Res. 2003; 44:218–224. [PubMed: 14660092]
13. Chabbra A, Tsuo D, Clark RT, et al. GDF-5 deficiency in mice delays Achilles tendon healing. J Orthop Res. 2003; 21:826–835. [PubMed: 12919870]
14. Palmes D, Spiegel HU, Schneider TO, et al. Achilles tendon healing: long-term biomechanical effects of postoperative mobilization and immobilization in a new mouse model. J Orthop Res. 2002; 20:939–946. [PubMed: 12382957]
15. Carpenter JE, Thomopoulos S, Soslowsky LJ. Animal models of tendon and ligament injuries for tissue engineering applications. Clin Orthop Relat Res. 1999; 367(Suppl):S296–S311. [PubMed: 10546654]
16. Wong J, Bennett W, Ferguson MW, et al. Microscopic and histological examination of the mouse hindpaw digit and flexor tendon arrangement with 3D reconstruction. J Anat. 2006; 209:533–545. [PubMed: 17005025]
17. Metsaranta M, Toman D, De Crombrugghe B, et al. Specific hybridization probes for mouse type I, II, III and IX collagen mRNAs. Biochim Biophys Acta. 1991; 1089:241–243. [PubMed: 2054384]
18. Yi Z, Cohen-Barak O, Hagiwara N, et al. Sox6 directly silences epsilon globin expression in definitive erythropoiesis. PLoS Genet. 2006; 2:129–139.
19. Hasslund S, Jacobson JA, Dadali T, et al. Adhesions in a murine flexor tendon graft model: autograft versus allograft reconstruction. J Orthop Res. 2008; 26:824–833. [PubMed: 18186128]
20. Hoffmann A, Pelled G, Turgeman G, et al. Neotendon formation induced by manipulation of the Smad8 signaling pathway in mesenchymal stem cells. J Clin Invest. 2006; 116:940–952. [PubMed: 16585960]
21. Wolfman NM, Hattersley G, Cox K, et al. Ectopic induction of tendon and ligament in rats by growth and differentiation factors 5, 6, and 7, members of the TGF-beta gene family. J Clin Invest. 1997; 100:321–330. [PubMed: 9218508]
22. Aoki H, Fujii M, Imamura T, et al. Synergistic effects of different bone morphogenetic protein type I receptors on alkaline phosphatase induction. J Cell Sci. 2001; 114(Pt 8):1483–1489. [PubMed: 11282024]
23. Schweitzer R, Chyung JH, Murtaugh LC, et al. Analysis of the tendon cell fate using Scleraxis, a specific marker for tendons and ligaments. Development. 2001; 128:3855–3866. [PubMed: 11585810]
24. Armstrong DG, Jude EB. The role of matrix metalloproteinases in wound healing. J Am Podiatr Med Assoc. 2002; 92:12–18. [PubMed: 11796794]
25. Tsubone T, Moran SL, Subramaniam M, et al. Effect of TGF-beta inducible early gene deficiency on flexor tendon healing. J Orthop Res. 2006; 24:569–575. [PubMed: 16463363]
26. Basile P, Dadali T, Jacobson J, et al. Freeze-dried tendon allografts as tissue-engineering scaffolds for Gdf5 gene delivery. Mol Ther. 2008; 16:466–473. [PubMed: 18180771]
27. Murchison ND, Price BA, Conner DA, et al. Regulation of tendon differentiation by Scleraxis distinguishes force-transmitting tendons from muscle-anchoring tendons. Development. 2007; 14:2697–2708. [PubMed: 17567668]

28. Brent AE, Schweitzer R, Tabin CJ. A somitic compartment of tendon progenitors. Cell. 2003; 113:235–248. [PubMed: 12705871]

29. Shukunami C, Takimoto A, Oro M, et al. Scleraxis positively regulates the expression of tenomodulin, a differentiation marker of tenocytes. Dev Biol. 2006; 298:234–247. [PubMed: 16876153]

30. Wang QW, Chen ZL, Piao YJ. Mesenchymal stem cells differentiate into tenocytes by bone morphogenetic protein (BMP) 12 gene transfer. J Biosci Bioeng. 2005; 100:418–422. [PubMed: 16310731]

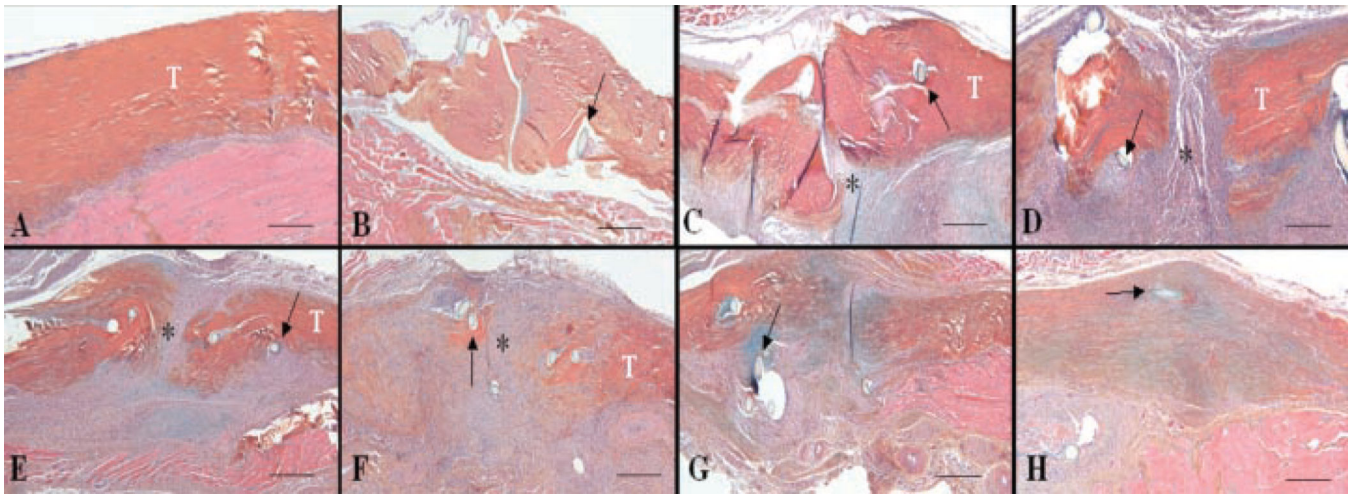


**Figure 1.**

Representative histology sections of normal (A) and repair FDL tendon at days 3 (B), 7 (C), 10 (D), 14 (E), 21 (F), 28 (G), and 35 (H) post-repair (4×). Sections were stained with Alcian Blue/Hematoxylin and OrangeG. Of note is the fibroblastic granulation tissue (*) that fills in the repair site between tendon ends (marked as T) (C–F) and is progressively remodeled with increasingly organized collagen fibers (F–H). Sutures are marked with arrows. Scale bars represent 25 μm.

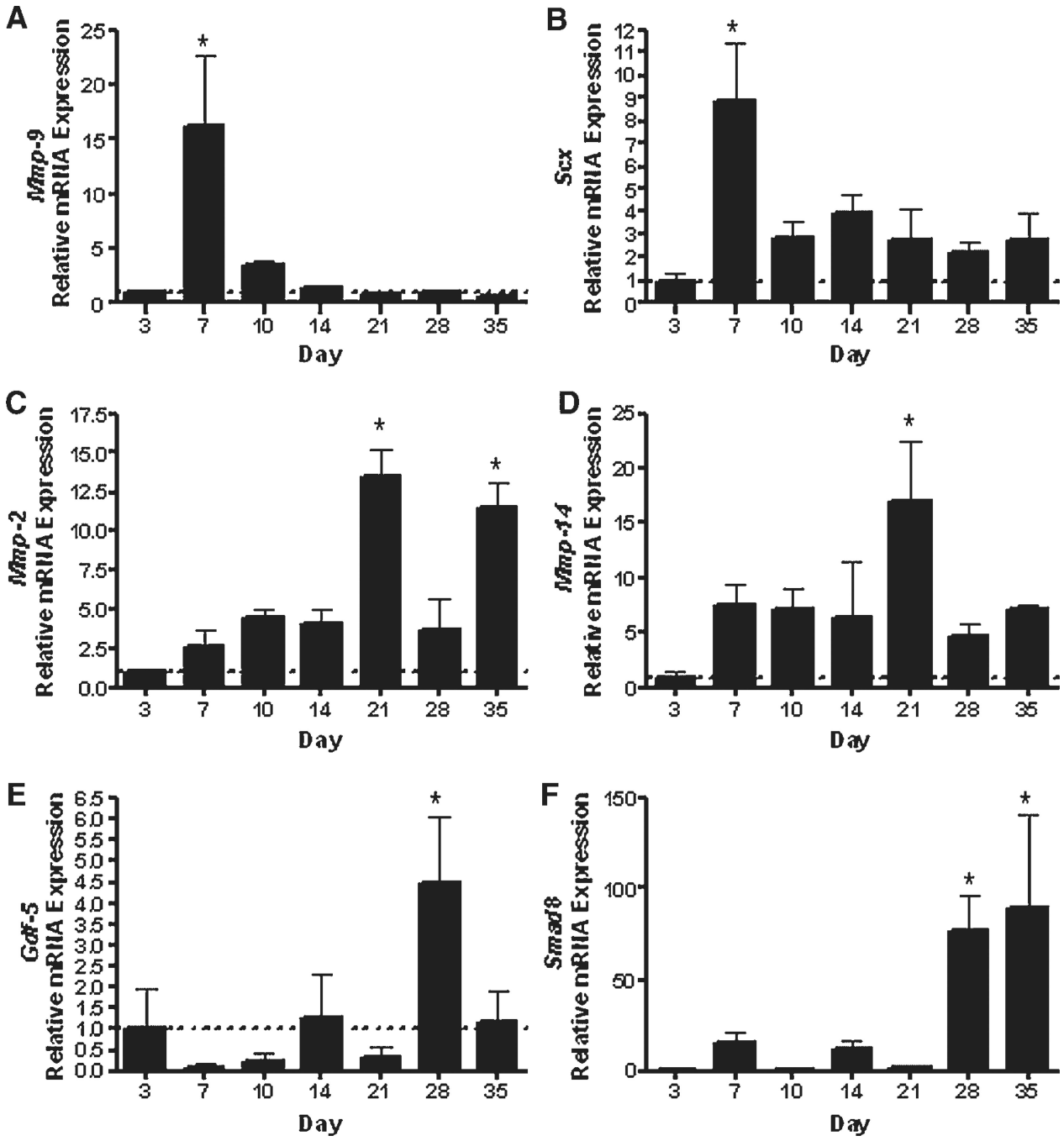


**Figure 2.**

Gene expression of (A) *Mmp-9*, (B) *Scx*, (C) *Mmp-2*, (D) *Mmp-14*, (E) *Gdf-5*, and (F) *Smad8* in FDL tendon repair tissue over time up to 35 days post-repair. Total RNA was extracted and pooled from five tendon repairs and processed for real-time RT-PCR. Gene expression was standardized with the internal β-*actin* control and then normalized by the level of expression in day 3 FDL tendon repairs. Data presented as the mean fold induction (over day 3 repairs) ± SD. *$p < 0.05$ versus day 3 tendon repair.

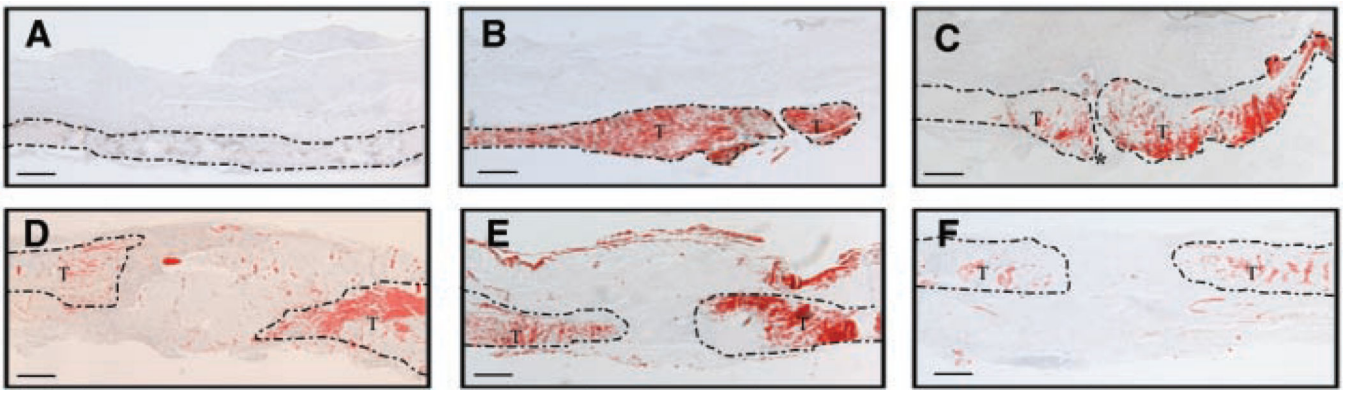


**Figure 3.**

In situ hybridization of *Scx* transcripts (Red) in normal tendon (A) and repair FDL tendons at days 3 (B), 7 (C), 10 (D), 14 (E), and 21 (F) (4×). Area of the tendon is outlined, and tendon tissue is marked as (T); granulation tissue is marked as (*). Scale bars represent 25 μm.

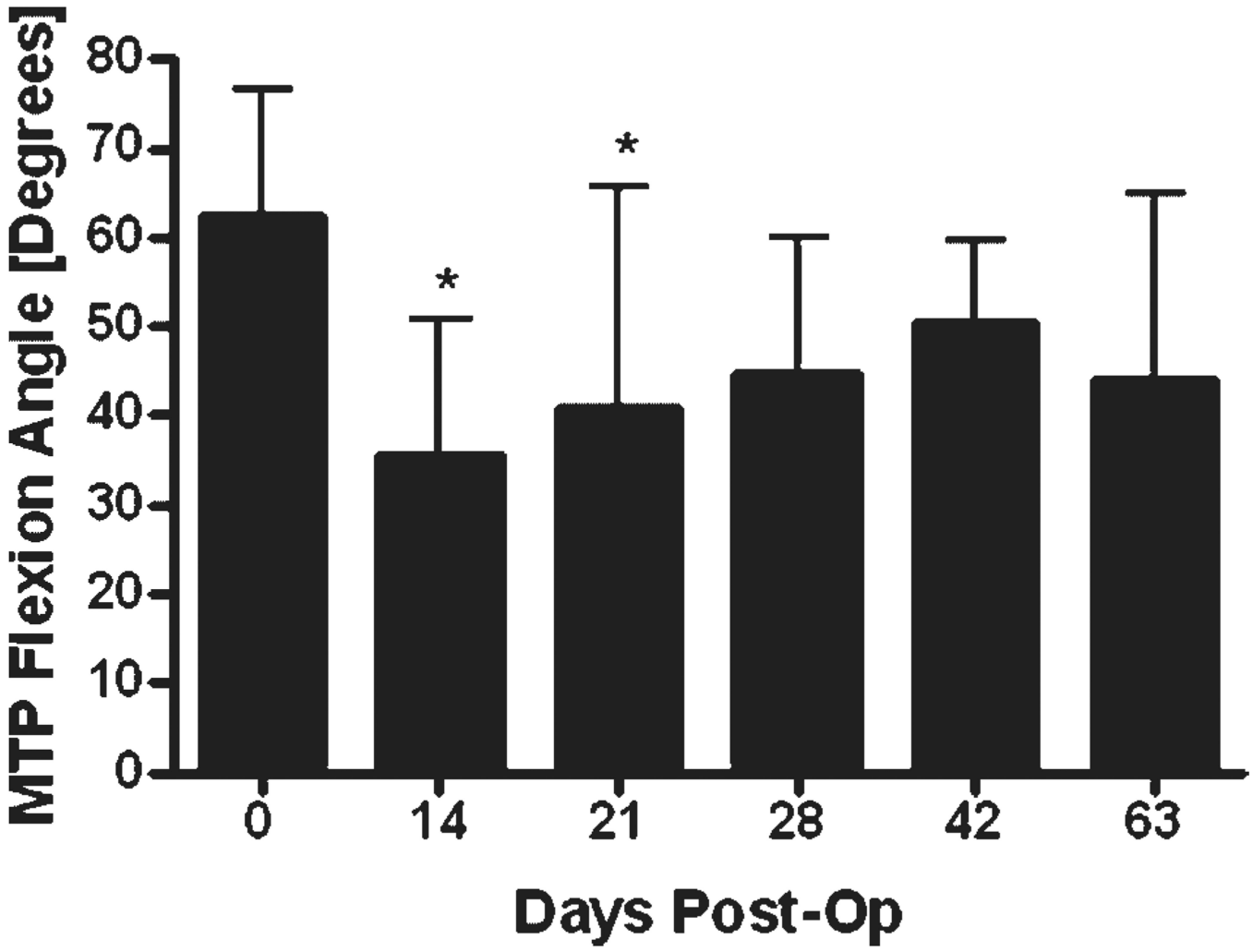


**Figure 4.**

MTP joint flexion ROM at the maximum applied load of 19 g of FDL tendon repairs at multiple time points post-repair (mean ± SD). Asterisk indicates significant difference versus day 0 operated tendons (Bonferroni's multiple comparison, $p < 0.05$).

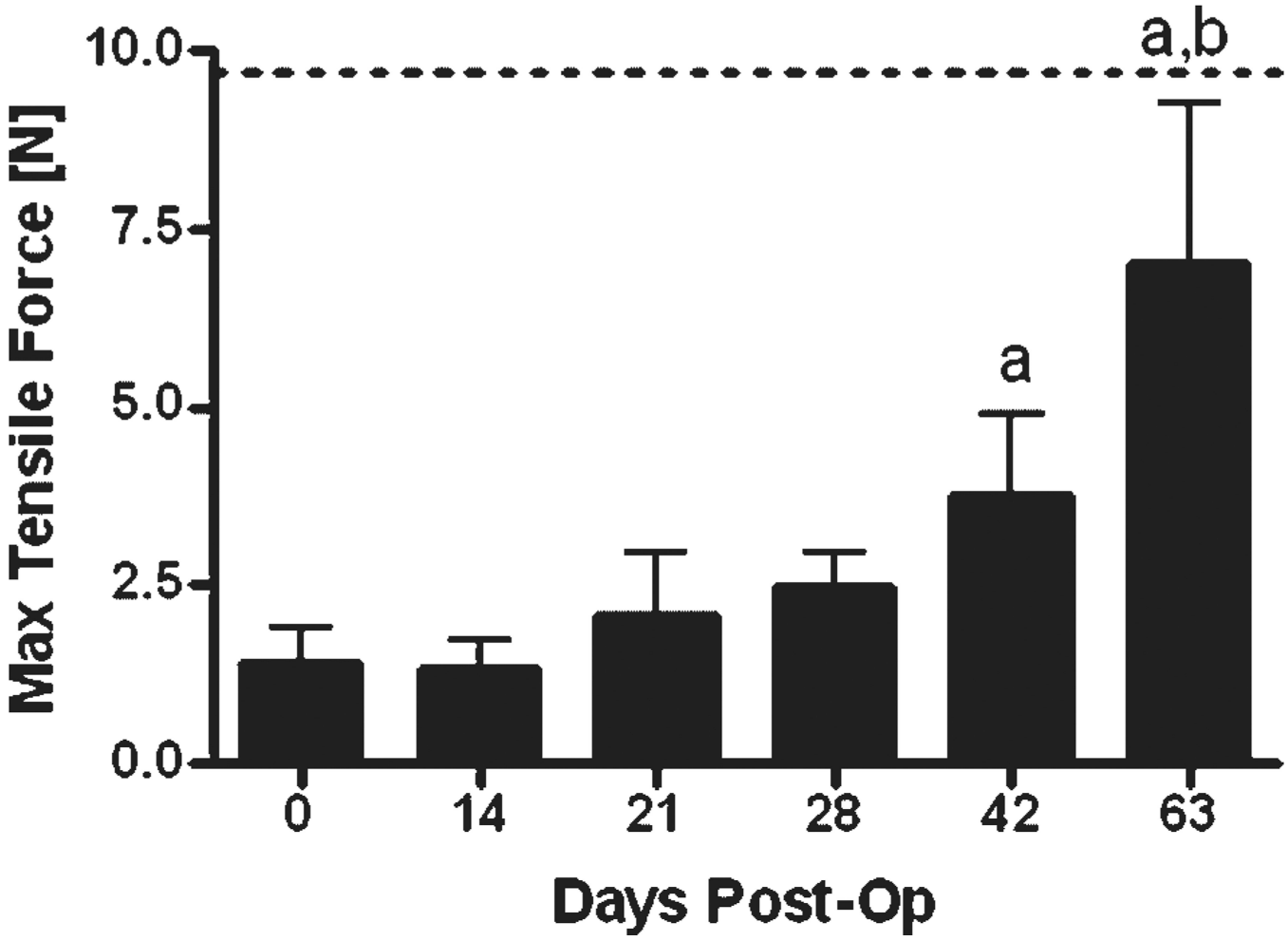


**Figure 5.**

Maximum tensile force of the FDL tendon repairs over time up to 63 days post-op, compared to day 0 repairs (mean ± SD). Label (a) indicates significant differences versus day 0; while label (b) indicates significant differences versus day 42. The dotted line represents the Max Tensile Force of un-operated tendon.

**Table 1**

Primer Sequences for Real-Time RT-PCR

| Gene | Forward Primer (5′ – 3′) | Reverse Primer (5′ – 3′) |
|---|---|---|
| *Col1a1* | GAGCGGAGAGTACTGGATCG | GCTTCTTTTCCTTGGGGTTC |
| *Col3a1* | GCC CAC AGC CTT CTA CAC | CCA GGG TCA CCA TTT CTC |
| *Scx* | TGGCCTCCAGCTACATTTCT | TGTCACGGTCTTTGCTCAAC |
| *Gdf-5* | GGCAAAGCATCTTCAAAAGC | CCAACTTCACGCTGCTGTTA |
| *Cox-2* | TGCAGAATTGAAAGCCCTCT | GCTCGGCTTCCAGTATTGAG |
| *Smad8* | GCC TAG CAA GTG TGT CAC CA | AGG CTG AGC TGA GGG TTG TA |
| *Mmp-2* | AGATCTTCTTCTTCAAGGACCGGTT | GGCTCCTCAGTGGCTTGGGGTA |
| *Mmp-9* | TGA ATC AGC TGG CTT TTG TG | ACC TTC CAG TAG GGG CAA CT |
| *Mmp-14* | GGATACCCAATGCCCATTGGCCA | CCATTGGGCATCCAGAAGAGAGC |
| β-*actin* | AGATGTGGATCAGCAAGCAG | GCGCAAGTTAGGTTTTGTCA |